Journal of Electroceramics, 11, 139–147, 2003

Surface Segregation Mechanisms in Ferroelectric Thin Films

B.E. WATTS,[1,*] F. LECCABUE,[1] G. TALLARIDA,[2] S. FERRARI,[2] M. FANCIULLI[2] & G. PADELETTI[3]

[1]*Istituto IMEM/CNR, Viale delle Scienze 37a, I-43100 Parma, Italy*

[2]*INFM, Laboratorio MDM, Via C. Olivetti 2, I-20041 Agrate Brianza, Italy*

[3]*Istituto ISMN/CNR, Via Salaria Km. 29,5, I-00016 Monterotondo Stazione (Roma), Italy*

Submitted February 25, 2003; Revised July 8, 2003; Accepted January 27, 2004

Abstract. Reliability issues have hampered the adoption of ferroelectric thin films by the microelectronics industry. One of these is imprint, an important problem affecting the performance of ferroelectric non-volatile memories. This paper presents the effects of the low temperature pyrolysis step on the chemical and physical properties of $SrBi_2Ta_2O_9$ films. A comparison of the hysteretic properties and composition profiles shows that control of the oxidising conditions during pyrolysis is critical to the dielectric properties. Data from this work and from the literature have been used to construct a model that explains the origin of surface depletion and segregation, self poling and as-grown imprint in ferroelectric films.

Keywords: ferroelectric, strontium bismuth tantalate (SBT), segregation, imprint, self poling

1. Introduction

Ferroelectric thin films, notably $Pb(Zr,Ti)O_3$ (PZT) and $SrBi_2Ta_2O_9$ (SBT), have been studied intensively over the last 15 years for a wide range of applications as sensors, microelectromechanical systems (MEMS), capacitors and non-volatile memories [1–3]. The ferroelectric effect has not been exploited extensively in devices till the realisation of ferroelectric random access memories (FeRAMs) [4, 5]. New research into the hysteretic properties has raised many issues that were considered unimportant or went unobserved in bulk ceramics. Nonetheless, they do affect the performance of thin film devices. Polarisation fatigue, retention and imprint are particularly important to the reliability of FeRAMS.

Imprint [6, 7] is a shift of the hysteresis curve along the field axis and prevents polarisation reversal. In operational FeRAMS it is caused by a continuous series of unipolar pulses or polarisation at higher temperatures. A voltage shift is also seen in the hysteresis loop of as grown films [8]. This may be caused by different interfacial effects at the top and bottom electrodes, moreover, the directional nature of the deposition process imposes non-centrosymmetric properties on the material.

There is a wealth of literature that describes the relationship between the ferroelectric properties, preparation method and film chemistry. The composition of an oxide film is rarely homogeneous through its thickness. Lead and bismuth diffuse into the bottom electrode and substrate, in addition, depleted layer of Pb and Bi is observed at the top surface. Evaporation of lead and bismuth, during the crystallisation of PZT and SBT, is given as the primary cause of depletion of these elements at the film surface. Although, the evidence for this is contradictory since the perovskite structure seems quite stable at temperature up to 700°C and there are many reports of lead and bismuth rich layers at the very surface [9, 10]. Clearly, correct models that explain the segregation of the components during the preparation of the film to predict the effects of processing in the film are needed.

Polli et al. [11] have shown that pyrolysis conditions are important to the production of homogeneous amorphous PZT powders from metallorganic precursors. The rate of hydrocarbon evolution during pyrolysis governs the local oxygen partial pressure during the reaction and a slow elimination of

*To whom all correspondence should be addressed. E-mail: watts@imem.bo.it

the carbonaceous suppressed the reduction to metallic Pb.

In this paper these considerations are applied to ferroelectrics thin films. Experiments on a series of SBT films pyrolysed using different thermal treatments before crystallisation are described. Evidence for surface segregation in $SrBi_2Ta_2O_9$ films, using composition profiles determined by secondary ion mass spectrometry (SIMS), is presented. The Bi composition profiles, together with literature data are used to construct model for surface diffusion. These can be applied to a range of multinary oxides of interest for microelectronic applications. They also help to understand the hysteretic properties of ferroelectric films, particularly the self-poling mechanism and imprint. Remedies to reduce the chemical segregation will be suggested.

2. Experimental

2.1. Preparation

The metallorganic decomposition (MOD) method used to prepare SBT has been published previously [12] but a brief description is necessary to help in the understanding of the discussion.

Strontium acetate, bismuth ethyl hexanoate and tantalum ethoxide were dissolved in acetic acid. An aliquot of diethanolamine was added to stabilise the solution. This precursor solution was syringed through a 0.2 μm filter onto 15 $\times$ 15 mm substrates and spun at 3000 rpm for 60 s. The structure of the substrate and electrode stack was: Si (001) (substrate)/SiO_2 thermally oxidised (100 nm)/TiN 20 nm/Pt sputtered 190 nm [13]. The baking step was done on a hot plate in air and/or in a tube furnace under flowing oxygen at 350°C between spins. The samples were inserted into a preheated furnace, under flowing oxygen. The different sequences of heat treatment with the exact times and temperatures used are listed in Table 1, along with the shorthand description used in this paper. Finally, the SBT was crystallised at 750°C in flowing oxygen for 1 h. A total of 4 layers were deposited after which the samples were heated to 750°C flowing oxygen to crystallise the Aurivillius phase, as confirmed by X-ray diffraction. The final thickness of crystallised SBT was approximately 0.2 μm.

Table 1. Heat treatments used for the low temperature baking step.

Heat treatment	Type/time (min)/temperature (°C)	Shorthand
1	Hot plate/15′/350	Single hot plate
2	Hot plate/15′/120 + hot plate/15′/350	Twin hot plate
3	Furnace /15′/350	Furnace

2.2. Chemical Analysis

Time-of-Flight Secondary Ion Mass Spectrometry (ToF-SIMS) depth profiles were acquired with a Cameca ION-TOF IV, equipped with two ion guns. A primary ion beam of Ga^+ gun operated with a current of 2.0 pA, with energy of 25 KeV and a pulse width of 800 ps was used for the analysis. The sputter gun was operated with O^{2+} at a voltage of 3 KeV and a current of 50 nA. Because of the insulating nature of SBT films a low energy electron flood gun was used to compensate the positive charge accumulating on the surface from the ion beam. O^{2+} sputtering was raster scanned over 150 $\times$ 150 μm, while Ga^+ analysis gun was raster scanned over 50 $\times$ 50 μm.

2.3. Electrical Measurements

Thin film capacitors were prepared by evaporating sputtering platinum through a metal mask. The dots were annealed in O_2 at 700°C for 30 mins, otherwise, the capacitor had low resistivity. Hysteresis was recorded with a modified Sawyer and Tower circuit [14] at a frequency of 1 kHz.

3. Results

3.1. Electrical Properties

The hysteresis loops for the three samples ("single hot plate," "twin hot plate" and "furnace" bake) are shown in Fig. 1. They are shifted downwards because individual capacitors tested for integrity and left in a poled state.

The "single hot plate" (Fig. 1(a)) treatment leads to the worst ferroelectric properties. The hysteresis loop is rounded, typical of films with high leakage currents and the polarisation relaxation is high. The "twin hot plate" (Fig. 1(b)) sample has a lower Pr (5 μC/cm^2) but saturates well; additionally, the coercive voltage is the

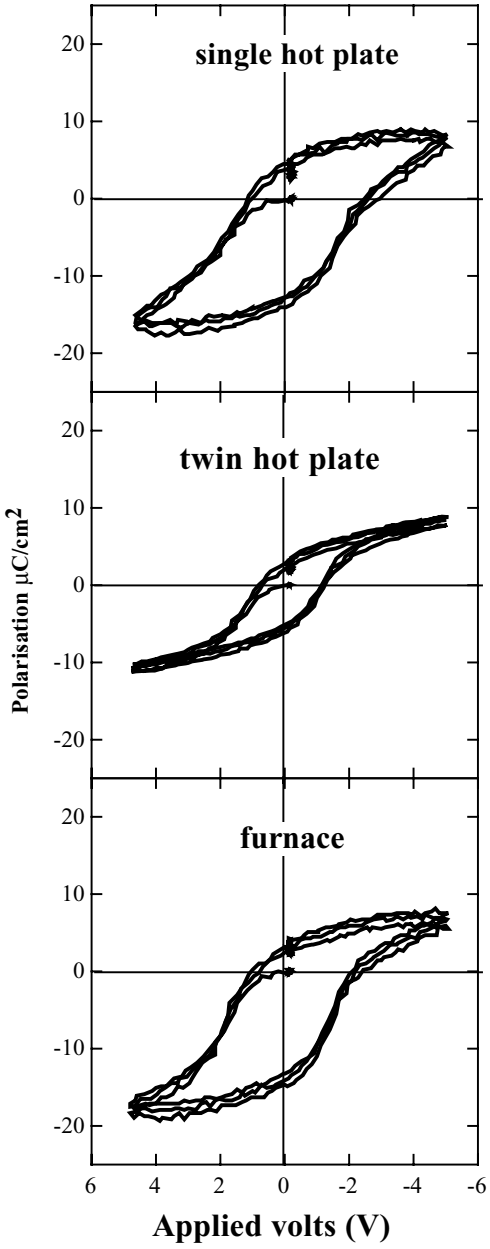

Fig. 1. SIMS profiles of Sr, Ta, Bi and Pt for the "twin hot-plate" film.

lowest of the three samples. The sample that underwent the "furnace" treatment (Fig. 1(c)) has the highest remnant polarisation (Pr), 6 and 7.5 μC/cm^2: moreover, the polarisation relaxation is small. The hysteresis loop in Fig. 2 is of a sample prepared on a 4″ diameter wafer in clean room conditions (class 1000). The baking conditions adopted were similar to the "furnace" treated sample but the slower heating rate that is imposed by the larger mass of substrate reflects on the electrical properties. The sample has a high remanent polarisation and low leakage as can be seen in the closed saturation. There is, however, a notable shift towards negative voltages (negative coercive voltage > positive coercive voltage). This is classical imprint in as grown material.

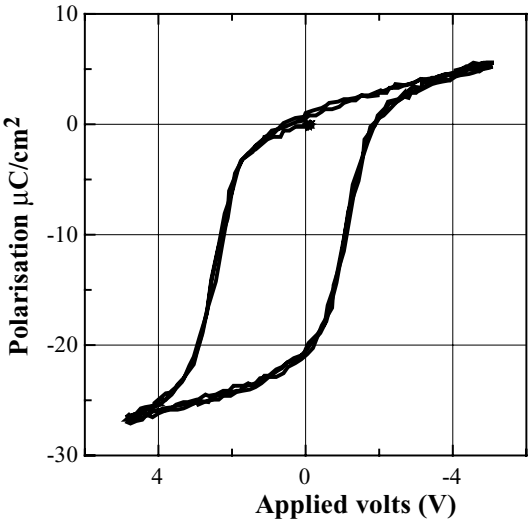

Fig. 2. SIMS profiles of Sr, Ta, Bi and Pt for the "furnace" film.

3.2. SIMS

Repeated runs showed that, "twin hot plate" and "furnace" samples gave consistently better results, hence, the samples made using these procedures were chosen for ToF-SIMS analysis. The beneficial effects of a two stage bake with respect to a single hot plate stage have been confirmed by other authors and is being adopted as best practice [15–17].

The SIMS composition profiles of the "twin hot plate" and "furnace" pyrolysis are presented in Figs. 3 and 4, respectively. It has been suggested that the high yields at the surface of ferroelectrics may be due to faster sputtering rates of Bi (or Pb) [18]. This is unlikely, as differences in sputtering rate are mainly due to differences in atomic weight. It would be reasonable to expect preferential sputtering of oxygen rather than bismuth or tantalum. Surface binding energy can also

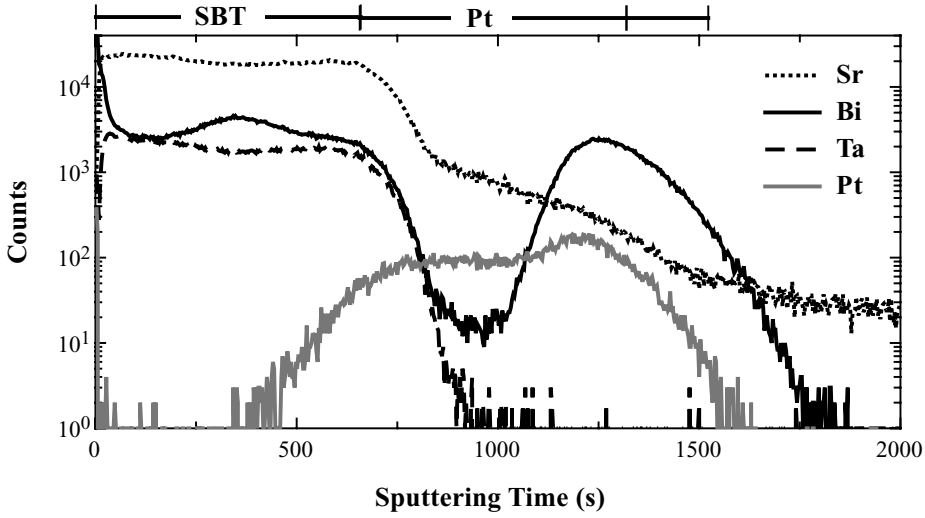

Fig. 3. Hysteresis loops of "single hot-plate", "twin hot-plate" and "furnace" films.

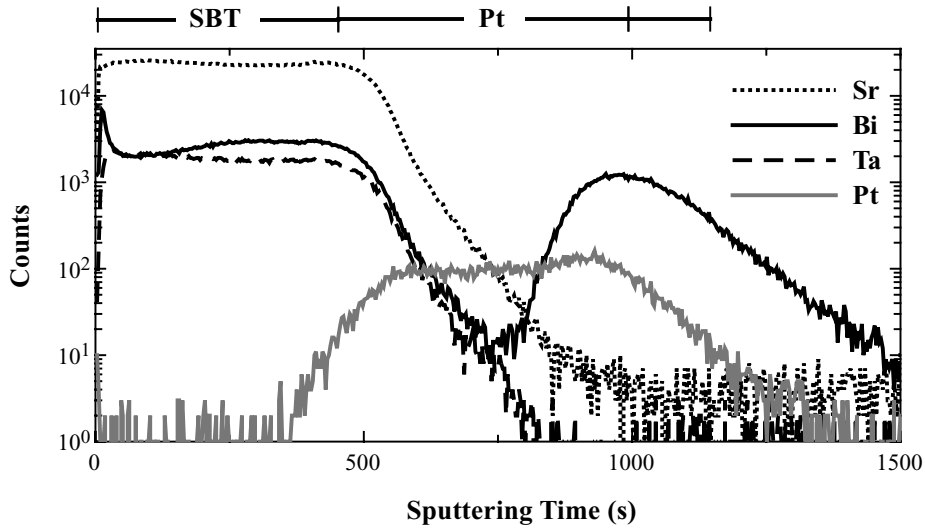

Fig. 4. Hysteresis loop of "furnace sample showing as grown imprint.

affect sputtering rates but this is a second order effect compared to that of the atomic mass.

SIMS profiles do not provide accurate quantitative analyses for the relative concentration of elements. Moreover, yields for an element change according to the matrix. But, the technique is sensitive to variations within a single phase. Surface enrichment on these samples was confirmed by Auger spectroscopy but SIMS results are presented since it is much more sensitive to surface layers.

4. Discussion

The pyrolysis experiments under different oxidising conditions show that the baking step is critical to the final electrical and structural properties of the film. Rapid heating can give porous films with a single step at 350°C and at least two steps are needed if fast thermal processing is desired. The biggest improvement in ferroelectric properties is seen on the "furnace" bake sample. This ensures better pyrolysis and less reduction

of the bismuth during the elimination of organic ligands.

The reduced bismuth that is present in the film has important consequences regarding its segregation both downwards into the substrate and towards the surface: Bi alloys with the platinum bottom electrode and diffuses towards the TiN buffer layer. The ToF-SIMS curves show that Bi has accumulated below the Pt in the region corresponding to the TiN buffer layer and is hardly present in the middle of the Pt. This is because in forming a compound with the Ti the chemical potential of the Bi is low [13]. Although ToF SIMS shows that this diffusion is not completely suppressed by the "furnace" bake, the bismuth concentration gradient in the SBT layer adjacent to the Pt is much flatter. This is A greater homogeneity is clearly desirable for microelectronic applications. Secondly, a bismuth peak can be seen in both samples, at the surface of the SBT film.

4.1. Surface Enrichment

The high concentration of bismuth at the surface of the SBT film is accompanied by a fall in Bi concentration immediately below the surface. Consequently, the relative Sr and Ta concentrations rise in the Bi depleted region. The "furnace" anneal gives a more homogeneous SBT film by containing the out-diffusion of the Bi.

The surface layer has been seen in SBT prepared by sputtering [19], MOCVD [20] and sol-gel [21]. XPS analysis has been able to reveal metallic Bi in SBT films along with severe surface enrichment [22].

An analogous Pb surface peak is commonly seen on the compositional profiles of PZT films. It has been observed using a variety of techniques including Rutherford backscattering (RBS) [18], Auger analysis [9, 23], and X-ray photoelectron spectroscopy (XPS) [10, 24]. Impey et al. [24] observed cyclic fluctuations in the Pb, Zr and Ti composition ratio through the five-layer film at depths that corresponded to the interfaces between the each layer, caused by a high pyrolysis temperature that leads to Pb segregation between each layer.

The structure of the surface oxide has been examined in details for PZT films. The high resolution transmission electron microscopy indicates that the PZT surface was covered with amorphous PbO and a small amount of nano-sized pyrochlore among the PZT grains [25]. An XPS depth profile analysis by Vasco et al. [10] of the Pb enriched near-surface region showed a strong decrease of the Pb/Ti ratio up to a depth of 12 nm. The same authors also report abroad PbO peak in the XRD spectra. Pb_3O_4 has been identified at the near surface region by XPS & Raman spectroscopy [26]. The fact that the surface layer is quite thin (10–20 nm) and is nanocrystalline, makes it difficult to reveal by simple XRD techniques.

This type of segregation is seen with other mutlicomponent oxides, not only in ferroelectrics. Bismuth containing pyrochlores also evidence this effect [27]. Tin diffuses to the surface of zirconium tin titanate prepared by sol-gel [28].

The loss of these metals in the films is a result of their diffusion towards the oxygen at the surface where they form nanocrystalline oxides, and hence are difficult to observe by normal X-ray diffraction (XRD) methods.

It is worth noting that once the ferroelectric has formed, the composition becomes stable, and the cations are tightly bound into the structure. The Pb concentration in PZT remains constant at higher temperatures and after a long annealing time [9], even in a vacuum [10].

4.2. Segregation Models

The presence of a Bi_2O_3 or PbO surface layer is intriguing since a continuous fall in Bi or Pb concentration would be expected up to the surface if evaporation were the cause of the surface depletion seen by many authors. Evaporation may take place at the surface of the bismuth oxide but it is not the origin of the depletion in the subsurface layer. We have commented that the pyrolysis influences the local oxygen partial pressure within the film, making subsequent annealing necessary to oxidise the film as well as to crystallise the SBT. The surface enrichment that leads to segregation of Bi is reminiscent of the cationic diffusion that takes in metal oxidation. Diffusion of metal cations towards the exposed oxide surface is commonly seen in metal corrosion and has been well described for copper [29–31].

The mechanism has been formulated by Wagner [32] and by Cabrera and Mott [33]. Figure 5 illustrates the case of a pure metal. The oxidation process begins with the adsorption and then chemisorption of oxygen from the ambient. Further oxidation can only take place if the metal, oxygen or point defects diffuse through the oxide. Generally, if the oxide is a defect semiconductor, it is not the oxygen that diffuses but the cations,

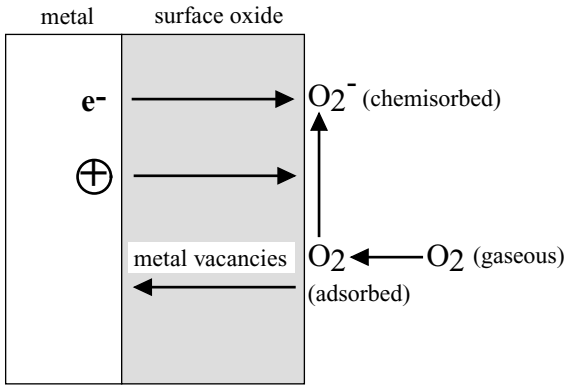

Fig. 5. Oxidation mechanism for a metal for the case when the cations diffuse faster than the oxygen.

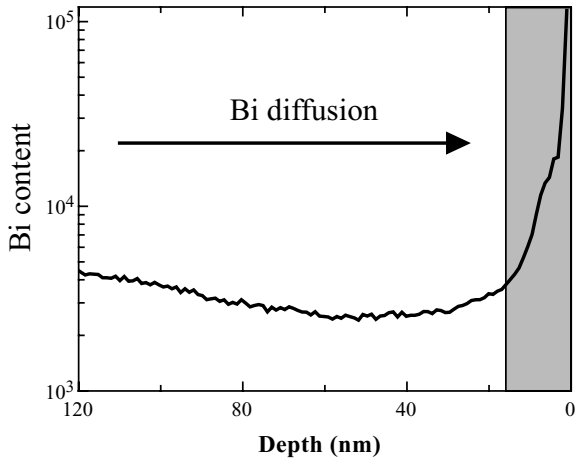

Fig. 6. Bismuth segregation down the electrochemical gradient.

e.g. for copper, tin, iron. At the initial stages of oxidation with a very thin oxide film the growth rate is very high. This is because there is a large electric field across the oxide, the Mott potential, which permits tunnelling of electrons from the metal to the surface. The thickness increases parabolically. As the oxide thickens the electrons no longer tunnel to the surface and the reaction slows. At higher temperatures a thermally activated process prevails and the kinetics also follow in a parabolic law for the dependence of film thickness versus time. This relationship can be derived assuming a linear decrease in metal concentration in the oxide.

Such oxidation mechanisms are not just limited to metals, but have also been invoked for simple oxides such as UO_2 [34].

The process is more intricate for a complex oxide; however, a qualitative description can be made. Bismuth, as the fastest diffusing element, migrates to the surface of the SBT where it oxidises to nanocrystalline Bi_2O_3 (Fig. 6). The curve superimposed on the diagram is of the Bi concentration curve in the "twin hot plate" SBT. Oxygen enters the lattice not as O^{2-} but as a cation vacancy that diffuses away from the surface. The first stages may be driven by a Mott potential but as the near surface loses Bi, the electric field is no longer sufficient and the reaction will only proceed by thermal activation. This extends the depleted layer to several tens of nanometers into the SBT.

Of course, this is a first simple model and the system is complicated by several factors. The ferroelectric layer undergoes several transformations from gel to xerogel, amorphous and then crystalline film. Each of these phases will behave differently in the oxygen atmosphere and any analysis will reflect the whole history of the sample. The SBT film may contain different phases such as the Aurivillius ferroelectric compound, Bi_2O_3, pyrochlore and fluorite. Diffusion takes place at grain boundaries rather than through the SBT grains.

Secondly, the properties of the surface oxide are different from that seen on a pure metal. It need not be coherent with the SBT film so oxygen can diffuse to the SBT surface. The surface is rough relative to the bismuth oxide thickness making it difficult to analyse and to determine the thickness of the Bi oxide layer quantitatively.

The model does give a plausible explanation for surface enrichment in multicomponent oxides.

4.3. Effects on the Ferroelectric Properties

Spurious phases on the surface will lessen the effective electric field applied to the ferroelectric and so increase the coercive field. The compositional changes across SBT itself affect the important dielectric properties (susceptibility, conductivity, polarisation). Two phenomena, self poling and imprint, induced by the composition gradient are discussed below.

4.3.1 Self Poling. A spontaneous polarisation is sometimes observed in ferroelectric films prepared by sol-gel, before applying any external electric field [24, 35–37]. This phenomenon is often associated with a propensity to pole more easily in one direction.

Impey et al. [24] report that PZT films have a built-in polarity and a propensity to pole electrically more easily in this vertical direction than the other. The polarisation direction induced indicated that the top surface was acting as the positive pole in the as deposited film. Similarly, Yamamoto et al. [36] observed self-polarisation with the same polarity and suggested that it is the cause of drift in the ferroelectric film but was unable to explain the origin of the polarisation.

The direction of growth imposed by deposition processes is expected to induce a preferential direction in the electrical properties, but this does not provide a mechanism for the polarity. The Cabrera and Mott model explains how an electric field can lead to drift of cations at the surface. Such fields would be sufficient to pole the material but it generally acts over the tunnelling distance of electrons in the growing oxide which is a few tens of nanometers. Secondly, direction of poling observed is the opposite of that which one would expect to be induced by the Mott field.

A field is generated by the diffusion of ions down the concentration gradient in the ferroelectric film. This is illustrated in Fig. 7. Pb^{2+} or Bi^{3+} diffuse faster than the oxygen anions which creates a field positive to negative into the film. This polarises the film as it cools through the Curie temperature. This is akin to the field gradient in a concentration cell but in this case the polarisation charge moves to compensate for the field. Once the ferroelectric polarisation is induced in the film, the diffusion accelerates and charge separation increases.

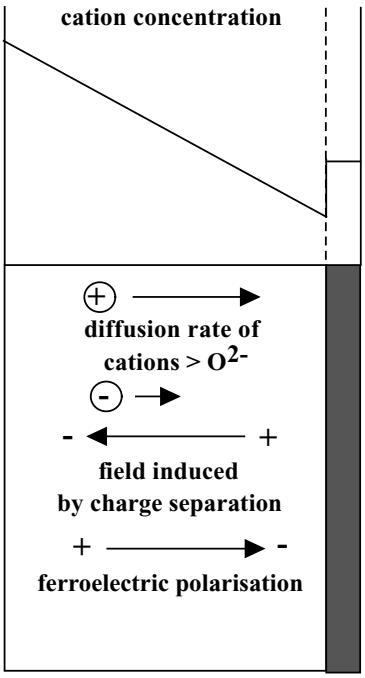

Fig. 7. Self polarisation mechanism resulting from the cation diffusion.

4.3.2 Imprint. Self-poling often goes unnoticed since the first few hysteresis cycles show leakage effects. Also, the film is subject to post processing when the electrodes are deposited and annealed that could depolarise the ferroelectric. This was not seen in SBT films in this work, but the hysteresis loop shown in Fig. 2 has a marked voltage shift towards negative voltages. The coercive voltages are lower in the positive direction, are as one would expect from the field polarity generated by the compositional gradient (Fig. 7).

As grown imprint has been reported in the literature for PZT. Okamura et al. [8] fabricated PZT thin films by a chemical solution deposition, which had an initial voltage shift in the P-E hysteresis loop toward the negative-bias field. The origin of the voltage shift was an internal bias field due to asymmetric space-charge distribution induced by the natural alignment of spontaneous polarization during the cooling process but no motive was given for the spontaneous polarisation. Interestingly, the mechanism for the voltage shift is the reverse of the one proposed in this paper.

An asymmetry of the P-E response was observed in Ni/PZT/Pt thin films [38] and was attributed to strong domain pinning near the top Ni electrode; domain pinning in the bulk of films does not play an important role. A larger value of dynamic pyroelectric response is obtained when the Ni/PZT/Pt film is positively pre-poled.

Imprint is present even when oxide electrodes are used. In the PZT/YBCO system there is a preferred polarization orientation in the ferroelectric PZT [37]. The defects present in the as-processed state of perovskite thin films, cation and O vacancies (Schottky defects) have the major role in creating an internal bias field causing the observed favoured orientation.

A point worth noting is the SIMS profile of the "twin hot plate" sample (Fig. 3) that has two opposing electrochemical gradients, both towards surface and substrate. This cancels or masks imprint but also decreases the switched polarisation.

4.4. Film Deposition Strategies

Various methods have been adopted to improve the imprint characteristics of ferroelectrics. Donor doping, e.g., replacing some of the Pb by La, is often used [3, 39, 40]. This is because of the lower oxygen vacancy concentration slows the Pb or Bi segregation. Rapid thermal processing (RTP) will always attenuate diffusion processes, acting to slow the oxidation process rather than the evaporation of volatile components. Rutherford back-scattering (RBS) data show that RTP maintains a better Pb stoichiometry than the conventional thermal process [9, 18]. Sometimes these approaches are not successful or give inconsistent results. The proposed oxidation model has implications for the preparation of ferroelectric thin films. Simple modifications to the deposition technique can be made to avoid segregation and imprint.

Ideally, the non-FE oxide layer on the surface would be eliminated completely if complete oxidation could be achieved before crystallisation. This should be done at low temperatures before there is any significant Pb or Bi diffusion. Higher oxygenation produced films with more symmetric hysteresis loops for PZT films prepared by sputtering [41]. The shift of the loops along the polarisation axis was ascribed to asymmetric leakage currents. However, a more fundamental understanding of the cause is gained from a consideration of the effect that oxygen vacancies have on the chemical distribution in the film. Similarly, SBT films prepared by sol gel had less imprint if they were put down thinner layers per spin, i.e. greater oxidation is achieved during each pyrolysis step [42].

Often, it is necessary to add Pb or Bi in excess, usually 10% above the formula stoichiometry, to prevent the crystallisation of the pyrochlore phase at the surface of ferroelectric thin. Evaporation is cited as the cause of the lower Pb or Bi, but the presence of a thin oxide layer at the surface conflicts with this hypothesis. The segregation model in this work suggests that it would be better to oxidise the film more effectively during the baking step and use near stoichiometric solutions for the preparation of FE thin films. A concentration gradient of those elements, which diffuse more readily, can set up an electrochemical potential to create the conditions that lead to imprint. Inoue et al. [40] found that excess Pb led to poorer electrical properties in this respect.

5. Conclusions

This work showed how the low temperature baking step is important to the final properties of the film affecting partitioning of the components and the dielectric properties.

The mechanisms of surface segregation in complex oxides have been described. These are similar to well known behaviour observed during the oxidation of metals. The model proposed explains the formation of a fine-grained oxide layer by diffusion of one component towards the exposed surface. In the case of lead or bismuth based ferroelectrics, this process leaves a region depleted in these elements immediately below the PbO and Bi_2O_3 layer. Hence, the depleted layer is not a direct result of evaporation losses at such low crystallisation temperatures (700°C).

These diffusion mechanisms provide the first explanation, for various phenomena observed in ferroelectric thin films.

(i) Self-polarisation is induced under particular pyrolysis conditions. The concentration gradient induces an electrical potential gradient that polarises the film when it cools below the Curie temperature. The spontaneous polarisation induced increases the surface enrichment.

(ii) This action of the electrochemical potential contributes to the asymmetry observed in the hysteretic properties known as imprint.

Further work is necessary to test and elaborate these hypotheses. In applying these criteria to film preparation it must be remembered that they should not be applied per se to a deposition process but must be accompanied by optimisation of the whole methodology including solution stoichiometry and heat treatments.

Acknowledgments

The authors thanks the Consiglio Nazionale delle Ricerche (CNR) for financial support.

References

1. J.F. Scott, C.A. Paz de Araujo, L. D. Macmillan, H. Yoshimori, H. Watanabe, T. Mihara, M. Azuma, T. Ueda, T. Ueda, D. Ueda, and G. Kano, *Ferroelectrics*, **133**, 47 (1992).
2. D.R. Uhlmann, J.T. Dawley, W.H. Poisi, and B.J.J. Zelinski, *Journal of Sol-Gel Science and Technology,* **19**, 53 (2000).

3. A.I. Kingon and S.K. Streiffer, *Curr. Opin. Solid State Mater. Sci.*, **4**, 39 (1999).
4. H. Takasu, *Journal of Electroceramics*, **4**, 327 (2000).
5. T. Sumi, Y. Judai, K. Hirano, T. Ito, T. Mikawa, M. Takeo, M. Azuma, S. Hayashi, Y. Uemoto, K. Arita, T. Nasu, Y. Nagano, A. Inoue, A. Matsuda, E. Fuji, Y. Shimada, and T. Otsuki, *Jpn. J. Appl. Phys.*, **35** (part 1, 2B), 1516 (1996).
6. W.L. Warren, B.A. Tuttle, D. Dimos, G.E. Pike, H.N. Al-Shareef, R. Ramesh, and J.T. Evans, *Jpn. J. Appl. Phys.*, **35**, 1521 (1996).
7. M. Grossman, O. Lohse, D. Bolten, U. Boettge, R. Waser, W. Hartner, M. Kastner, and G. Schindler, *Appl. Phys. Lett.*, **76**, 363 (2000).
8. S. Okamura, S. Miyata, Y. Mizutani, T. Nishida, and T. Shiosaki, *Jpn. J. Appl. Phys.*, **38** (part 1, no. 9B), 5364 (1999).
9. S.S. Dana, K.F. Etzold, and J. Clabes, *J. Appl. Phys.*, **243**, 4398 (1991).
10. E. Vasco, O. Böhme, E. Romàn, and C. Zaldo, *Appl. Phys Lett.*, **78**, 2037 (2001).
11. A.D. Polli and F.F. Lange, *J. Am. Ceram. Soc*, **78**, 3401 (1995).
12. B.E. Watts, F. Leccabue, M. Fanciulli, S. Ferrari, G. Tallarida, D. Parisoli, and C. Morandi, *Integrated Ferroelectrics*, **37**, 565 (2001).
13. B.E. Watts, F. Leccabue, S. Guerri, M. Severi, M. Fanciulli, S. Ferrari, G. Tallarida, and C. Morandi, *Thin Solid Films*, **406**, 23 (2002).
14. P. Falchetti, Thesis, Engineering Department, Universiy of Parma, Italy (2002).
15. Y. Fujisaki, K. Iseki, and H. Ishiwara, *Jpn. J. Appl. Phys.*, **42** (part 2, no. 3B), 267 (2003).
16. Z.-J. Wang, R. Maeda, and K. Kikuchi, *Jpn. J. Appl. Phys.*, **38**, 5342 (1999).
17. M. Kosec, B. Malic, and M. Mandeljc, *Mater. Sci. Semicond Process*, **2/3**, 97 (2002).
18. R. Sirera, D. Leinen, E. Rodríguez-Castellón, and M.L. Calzada, *Chem. Mater.*, **11**, 3437 (1999).
19. Y.-B. Park, S.-M. Jang, J.-K. Lee, and J.-W. Park, *J. Vac. Sci. Technol. A,* **18**, 17 (2000).
20. N.-J. Seong and E.-S. Choi, *J. Vac. Sci. Technol. A*, **17**, 83 (1999).
21. C.H. Lu and B.K. Fang, *J. Mat. Res.*, **12**, 2104 (1997).
22. S. Ono, A. Sakakibara, T. Osaka, I. Koiwa, J. Mita, and K. Asami, *J. Electrochem. Soc*, **146**, 685 (1999).
23. K.M. Lee, H.G. An, J.K. Lee, Y.T. Lee, S.W. Lee, S.H. Joo, S.D. Nam, K.S. Park, M.S. Lee, M.S. Park, H.K. Kang, and J. T. Moon, *Jpn. J. Appl. Phys.*, **40**, 4979 (2001).
24. S.A. Impey, Z. Huang, A. Patel, R. Beanland, N.M. Shorrocks, R. Watton, and R.W. Whatmore, *J. Appl. Phys*, **83**, 2202 (1998).
25. G.-S. Park and I.-S. Chung, *Jpn. J. Appl. Phys.*, **41**, (part 1 no. 3A), 1519 (2002).
26. Y.-C. Lai, Y.S. Gong, and C. Lee, *Mater. Chem. Phys.*, **51**, 147 (1997).
27. A.K. Bhattacharya, S.F. Forster, D.R. Pyke, K.K. Mallick, and R. Reynolds, *J. Mater. Chem.*, **7**, 837 (1997).
28. G. Gusmano, A. Bianco, M. Viticoli, S. Kaciulis, G. Mattogno, and L. Pandolfi, *Surf. Interface Anal.*, **34**, 690 (2002).
29. S.K. Roy, S.K. Mitra, and S.K. Bose, *Oxidation of Metals*, **49**(3/4), 261 (1998).
30. R. Haugsrud and P. Kofstad, *Oxidation of Metals*, **50**(3/4), 189 (1998).
31. M. Martin and E. Fromm, *J. Alloy Comp.*, **258**, 7 (1997).
32. C. Wagner, *Z. Phys. Chem., B*, **21**, 25 (1933).
33. N. Cabrera and N.F. Mott, *Rep. Prog. Phys.*, **12**, 163 (1948).
34. R.J. McEachern and P. Taylor, *J. Nucl. Mater.*, **254**, 87 (1998).
35. K.S. Sumi, H. Qiu, M. Shimada, S. Sakai, and T. Nishiwaki, *Jpn. J. Appl. Phys.*, **38**, 886 (1999).
36. T. Yamamoto, J. Sakamoto, E. Matuzaki, and R. Takayama, *Jpn. J. Appl. Phys.*, **38** (part 1, no. 9B), 5332 (1999).
37. A.R. Zomorrodian, N.J. Wub, H. Linb, and A. Ignatiev, *Thin Solid Films*, **335**, 225 (1998).
38. W. Liu, J. Ko, and W. Zhu, *Mater. Lett.*, **49**, 122 (2001).
39. M. Shimizu, H. Fujisawa, and T. Shiosaki, *Microelectronic Engineering*, **29**, 173 (1995).
40. N. Inoue, T. Takeuchi, and Y. Hayashi, *IEEE Trans Electron Dev*, **49**(9), 1572 (2002).
41. G. Poullain, R. Bouregba, B. Vilquin, G. Le Rhun, and H. Murray, *Appl. Phys Lett.*, **81**, 5015 (2002).
42. K. Okuwada and M. Saito, *Electron Comm Jpn*, **8**, 40 (2001).